Available online at www.sciencedirect.com

SciVerse ScienceDirect

Ceramics International 39 (2013) 5937–5941

CERAMICS INTERNATIONAL

www.elsevier.com/locate/ceramint

Short communication

Fabrication and properties of 3-D C_f/ZrB_2–ZrC–SiC composites via polymer infiltration and pyrolysis

Qinggang Li[a,*], Shaoming Dong[b,*], Zhi Wang[a], Guopu Shi[a]

[a]School of Material Science and Engineering, University of Jinan, Jinan 250022, China

[b]Structural Ceramics and Composites Engineering Research Center, Shanghai Institute of Ceramics, Chinese Academy of Sciences, Shanghai 200050, China

Received 12 November 2012; received in revised form 24 November 2012; accepted 25 November 2012
Available online 5 December 2012

Abstract

Three-dimensional needled C_f/ZrB_2–ZrC–SiC composites were successfully fabricated via polymer infiltration and pyrolysis (PIP) using ZrB_2 powder, polycarbosilane, and ZrC precursor as raw materials. The microstructures and mechanical properties of the composites were studied using X-ray diffraction, scanning electron microscopy and the three-point bending test. Their high-temperature oxidation resistance and anti-ablation properties were evaluated using a muffle furnace and plasma wind tunnel test. Results show that the composites have good mechanical and excellent ablative properties.

Keywords: C. Mechanical properties; Ceramic–matrix composites; ZrC precursor; High-temperature properties

1. Introduction

As structural materials, carbon fiber-reinforced silicon carbide matrix (C_f/SiC) composites are limited because of their thermal stability in high-temperature oxidizing environments below 1600 °C. C_f/SiC composites are resistant to oxidation up to 1600 °C because of the protective SiO_2 surface film, which is an excellent oxidation barrier for environments below 1600 °C. However, it begins to soften dramatically and develop substantial vapor pressure at temperatures above 1600 °C [1–4]. With the development of hypersonic aerospace vehicles and advanced reusable atmospheric re-entry vehicles, C_f/SiC composites can no longer withstand ablation environments with high heat flux and pressure gas flows.

Recently, much work has been done to improve the high-temperature performance and anti-ablation properties of C_f/SiC composites. Currently, two potential approaches may be applied to develop fiber-reinforced ceramic composites that perform at ultra-high temperatures (>1600 °C) under oxidative conditions. These approaches include (a) fabrication of ultra-high-temperature ceramic (UHTC) coatings on the surfaces of carbon-fiber-reinforced carbon–matrix composites (C/C) or C/SiC composites, and (b) the introduction of UHTCs into the matrix. To fabricate UHTC coatings, Zhou et al. prepared ZrB_2–SiC oxidation protective coatings on C/C composite via the vapor silicon infiltration process [5]. Many papers [6–9] have revealed that C_f/UHTCs composites can be fabricated by introducing UHTCs into the matrix. Much work on the ZrB_2–SiC system has been done [10–16]. However, only Zhang et al. [14] and Zhang et al. [16] fabricated ZrB_2–SiC–ZrC composites via hot pressing and reactive hot pressing and investigated their microstructural features and mechanical properties. NASA has reported that the performances of ZrB_2/ZrC/SiC composites are superior to those of ZrB_2/SiC or HfB_2/SiC composites. [17,18] Therefore, we will try to introduce ZrB_2/ZrC/SiC into the matrix to improve the high-temperature performance of C_f/SiC composites. Until now, nothing has been reported on C_f/ZrB_2–ZrC–SiC composites.

Based on our previous study, the present work aims to develop a new ternary ceramic matrix for the fabrication of three-dimensional (3-D) C_f/ZrB_2–ZrC–SiC composites.

*Corresponding authors.
E-mail addresses: liqinggang66@gmail.com (Q. Li), smdong@mail.sic.ac.cn (S. Dong).

0272-8842/$ - see front matter © 2012 Elsevier Ltd and Techna Group S.r.l. All rights reserved.
http://dx.doi.org/10.1016/j.ceramint.2012.11.074

In this communication, we report our initial studies on the preparation of 3-D C_f/ZrB_2–ZrC–SiC composites using ZrB_2 powder, polycarbosilane, and ZrC precursor as raw materials. The mechanical and high-temperature properties of the composites were also studied.

2. Experimental procedure

Carbon fibers (T300SC, Toray, Tokyo, Japan) with an average diameter of 6 μm were used. The 3-D fabrics were manufactured by Nanjing Fiberglass Research and Design Institute (Nanjing, China). The architecture had a fiber distribution of 8:2:1 in the *x*:*y*:*z* directions, respectively, and an ~40% fiber volume fraction. Some 3-D fabrics were coated with PyC or PyC/SiC interphase via chemical vapor infiltration. ZrB_2 powder (~10 μm, >90 wt% pure, Dandong Chemical Co. Ltd., Dandong, China), ZrC precursor (Institute of Process Engineering, Chinese Academy of Science), and PCS (National University of Defense Technology, Changsha, China) were first ball milled at a volume ratio of 64:16:20 to form a homogenously dispersed slurry using xylene as solvent. Recently Li et al. [8,9] reported the nature of the PZC precursor. The 3-D fabrics were then impregnated by the above-mentioned slurry. Thereafter, the samples were dried in a 120 °C rotating evaporator and pyrolyzed in a 900 °C hot-pressing furnace with inert gas to form 3-D C_f/ZrB_2–ZrC–SiC composites. The obtained composites were further densified via four cycles of the polymer infiltration and pyrolysis (PIP) process and then heated at 1500 °C in a high-temperature graphite resistance furnace at a rate of 10 °C/min to open the closed pores.

The densities of the samples were measured using the Archimedes method. The samples were cut into 4 mm × 5 mm × 60 mm specimens and polished for the three-point bending test in an Instron-5566 testing machine with a crosshead speed of 0.5 mm/min and a span of 48 mm. The phase compositions of the composites were characterized by X-ray diffraction (XRD) with Cu K_α radiation. The microstructures of the composites were studied using an Electron Probe Micro-analyzer (EPMA, JXA-800, Jeol, Tokyo, Japan) equipped with an energy-dispersive spectrum (EDS, INCA, Oxford, Tokyo, Japan).

A high-temperature oxidation test was conducted in a muffle furnace. After oxidation, the phase compositions of composites were characterized by XRD with Cu K_α radiation. The anti-ablation test was performed in a plasma wind tunnel. During the test, the specimen with a size of 80 mm × 80 mm × 10 mm was vertically exposed to the flame for 300 s when the surface temperature of the composite reached 2300 K. The distance between the nozzle tip and the surface of the specimen was 10 mm and the inner diameter of the nozzle tip was 2.0 mm.

3. Results and discussions

The physical and mechanical properties of the 3-D C_f/ZrB_2–ZrC–SiC composites with different interphases are summarized in Table 1. As shown, the samples without interphases have higher densities (2.44 g/cm^3). However, their open porosities were only slightly different. The composites with PyC/SiC interphases between fiber and matrix have a bulk density of 2.28 g/cm^3, open porosity of 13%, and bending stress of 248 MPa. The existence of interphases (PyC or PyC/SiC) prevents UHTC phases from going through the wrapped bundles during the impregnation process. Hence, composites without interphases have more UHTCs and thus, higher densities.

Table 1
Physical and mechanical properties of 3-D C_f/ZrB_2–ZrC–SiC composites with different interphases.

Interphase	Fiber fraction (vol%)	UHTCs fraction (vol%)	Density (g/cm^3)	Open porosity (%)	Bending stress (MPa)	Elastic modulus (GPa)
None	34	30	2.44	12	136 ± 27	20 ± 3.0
PyC	33	25	2.27	15	196 ± 30	26 ± 3.0
PyC/SiC	33	23	2.28	13	248 ± 28	28 ± 4.0

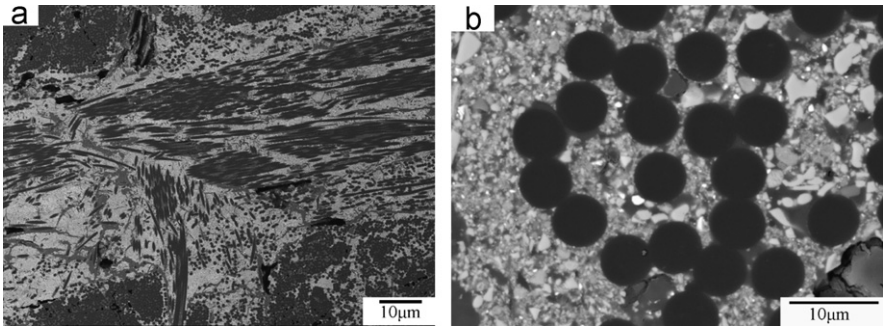

Fig. 1. Back-scattered electron images for the polished cross sections of 3-D C_f/ZrB_2–ZrC–SiC composites: (a) back-scattered electron image; and (b) larger magnification.

As shown by the micrographs of the polished cross sections of composites with interphases (Fig. 1), the areas between the fiber bundles (Fig. 1a) as well as the fiber tows inside (Fig. 1b) are filled with slurry. The UHTCs are almost evenly distributed in the interbundle matrix, but some pores are evident in the intrabundle areas. Numerous volatile gases evaporate during the high-temperature pyrolysis of the polymer precursor. This evaporation produces the diffusion channels along with some pores for further composite densification via PIP. The EDS analysis (Fig. 2) shows that the matrix in the interbundle areas has a composition of B, C, O, Si, and Zr. Their fillers are believed to be ZrB_2, ZrC, and SiC. Moreover, the composition contains some oxygen resulting from the oxidation of ZrB_2, ZrC precursor, and PCS. The UHTC phase is dispersed homogenously in the composites, with ZrC and ZrB_2 phases having white backgrounds in the backscattered electron micrographs and SiC phases having dark background.

The typical bending stress–displacement curves of all composites with different interphases are shown in Fig. 3. These curves show that all samples exhibit typical non-catastrophic fracture behaviors regardless of the existence of interphases. With the interphase depositions, the mechanical properties, including the elastic modulus and bending force, are increased. This result is consistent with the data listed in Table 1.

The morphologies of the fracture surfaces are shown in Fig. 4. Consistent with the typical nonbrittle fracture behavior revealed by the bending stress–displacement curves, all composites exhibited fiber pull-outs during the fracture process. When no interphase is deposited, the pulled-out fibers are short and their surfaces are rather coarse. In contrast, with PyC/SiC or PyC interphases, the pulled-out fibers are longer and their surfaces are smoother. This phenomenon can be explained by the bonding strength between the fibers and matrix. When no interphase exists, a strong-bonding interface is produced when the composites are heated at high temperature. Therefore, the matrix cracks tend to penetrate into the fibers directly with no crack deflection. On the contrary, when the PyC/SiC or PyC interphases are deposited, the interphases result in a weak bonding between the fibers and matrix, facilitating crack deflection and fiber pull-out, which are beneficial to the improvement of fracture toughness.

The high-temperature property of the C_f/UHTC composite is important. Hence, the 3-D C_f/ZrB_2–ZrC–SiC composite was evaluated via high-temperature oxidation resistance and a plasma wind tunnel test. Fig. 5 shows the morphologies of the 3-D C_f/ZrB_2–ZrC–SiC composite before (Fig. 5a), and after (Fig. 5b) anti-oxidation and during the anti-ablation property test (Fig. 5c). Fig. 4a shows the original morphology and XRD pattern of the composite. As shown by the diffraction peaks, the main

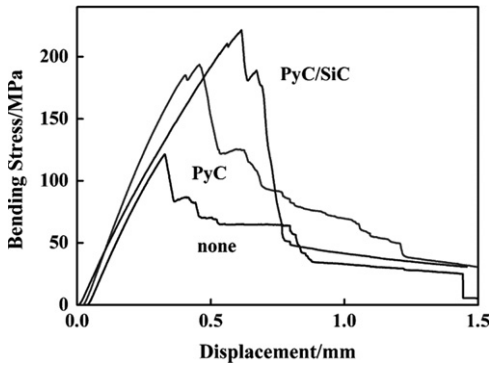

Fig. 3. Bending stress/displacement curves of 3-D C_f/ZrB_2–ZrC–SiC composites with different interphases.

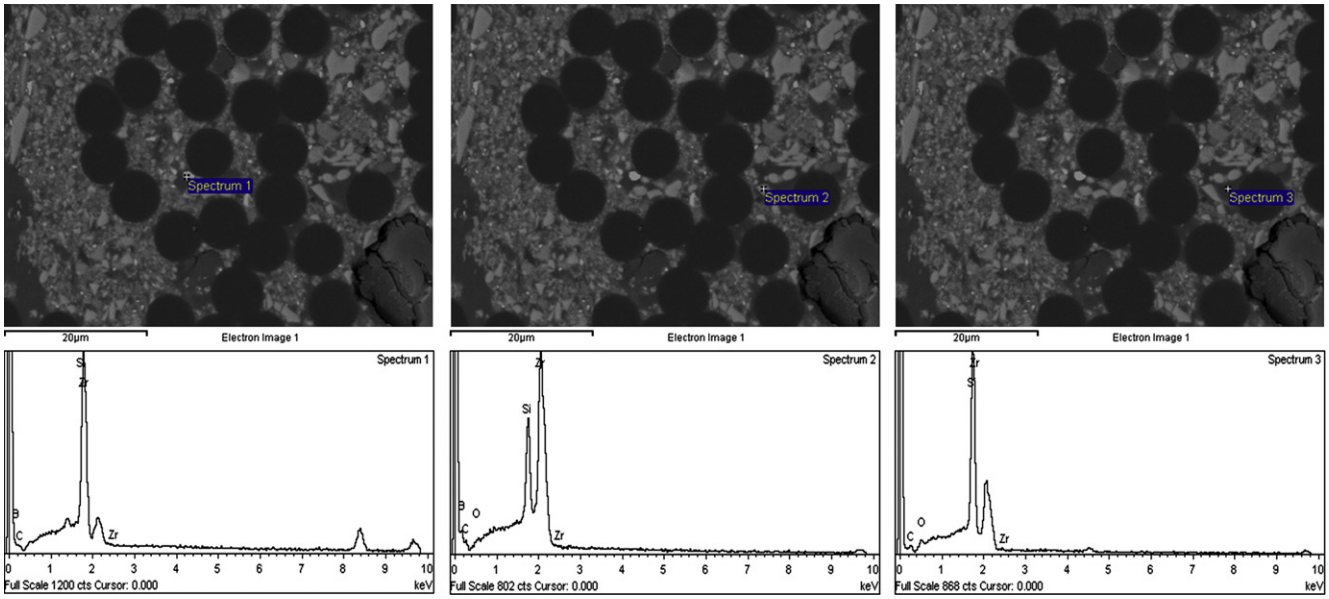

Fig. 2. Electron probe microscopy micro analyzer micrographs and energy-dispersive spectrum analysis of 3-D C_f/ZrB_2–ZrC–SiC composites.

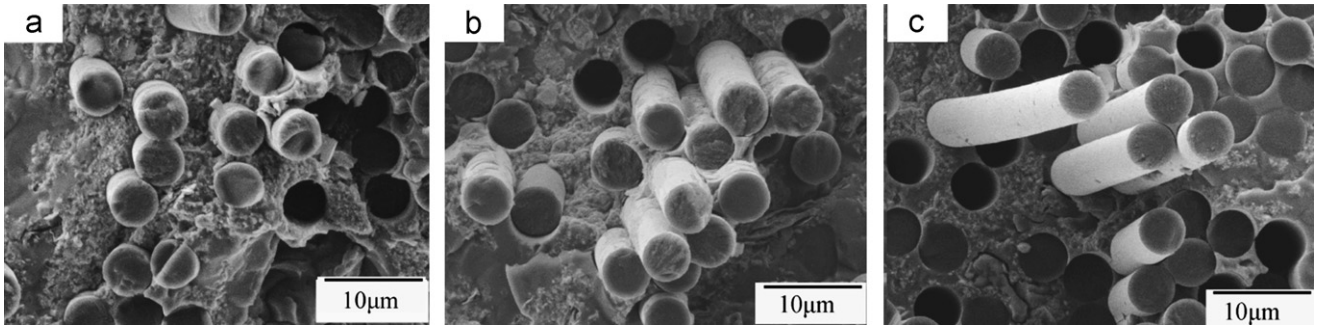

Fig. 4. SEM micrographs on the fracture surfaces of 3-D C_f/ZrB_2–ZrC–SiC composites: (a) none; (b) PyC; and (c) PyC/SiC.

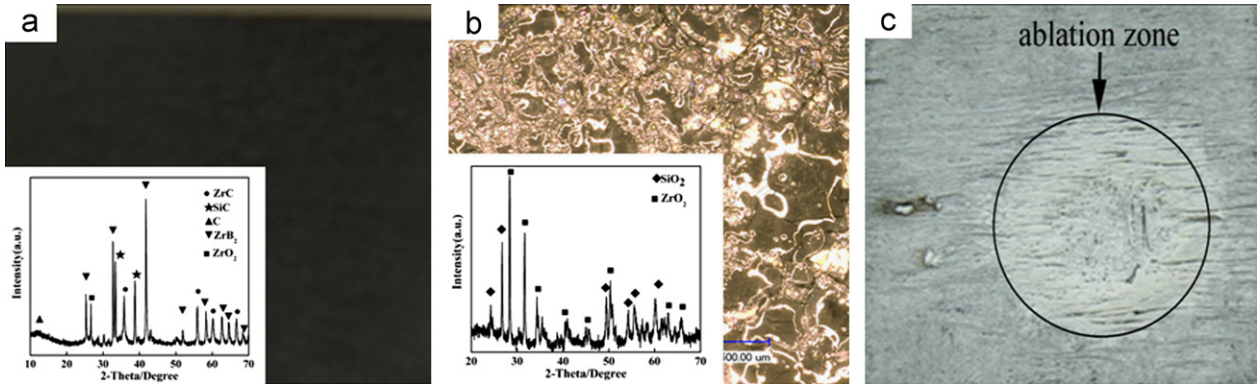

Fig. 5. Morphologies of 3-D C_f/ZrB_2–ZrC–SiC composite after anti-oxidation and anti-ablation property test: (a) original morphology; (b) morphology after oxidation; and (c) morphology after ablation.

phases existing in the composite are ZrB_2, ZrC, SiC, and ZrO_2. The results validate the EDS analysis of the polished cross-sectional surface.

Fig. 5b shows the morphologies of the 3-D C_f/ZrB_2–ZrC–SiC composite after oxidation at 1700 °C for 15 min in a high-temperature muffle furnace. The XRD pattern of the composite surface after oxidation is shown in Fig. 5b. According to Fig. 5b, a glass layer of SiO_2 and ZrO_2 is formed when the composite is used in the oxidative atmosphere. This glass layer prevents the composite from further oxidation. And after the anti-oxidation test, the samples increase their weight. Fig. 5c shows the morphologies of the 3-D C_f/ZrB_2–ZrC–SiC composite after the ablation test. From the ablation zone, the composite almost remains intact after ablation. The mass loss and linear recession rate of the 3-D C_f/ZrC–SiC composite tested via a plasma wind tunnel were 0.010 g/s and 0.002 mm/s, respectively. Thus, 3-D C_f/ZrB_2–ZrC–SiC composites have good oxidation resistance and excellent high-temperature properties.

4. Conclusions

The 3-D C_f/ZrB_2–ZrC–SiC composites were fabricated via PIP with ZrB_2, polycarbosilane, and ZrC precursor as raw materials. All composites exhibit the typical non-brittle fracture behavior. The composites with PyC/SiC interphases have a bulk density of 2.28 g/cm^3, open porosity of 13%, and bending stress of 248 MPa. The composites also have good oxidation resistance and excellent high-temperature properties.

Acknowledgments

Authors appreciate the financial support of the National Natural Science Foundation of China under the Grant no. 51172256 and the Grant no. 51142010. Authors also thank Professor Xiaolei Wu and Professor Heji Huang from the Institute of Mechanics Chinese Academy of Sciences for the plasma wind tunnel test.

References

[1] S. Schmidt, S. Beyer, H. Knabe, H. Immich, R. Meistring, A. Gessler, Advanced ceramic matrix composite materials for current and future propulsion technology applications, Acta Astronautica 55 (2004) 409–420.
[2] W. Krenkel, B. Heidenreich, R. Renz, C/C–SiC composites for advanced friction systems, Advanced Engineering Materials 4 (2002) 427–436.
[3] R.L. Stanley, J.O. Elizabeth, C.H. Michael, D.K. James, S. Mrityunjay, A.S. Jonathan, Evaluation of ultra-high temperature ceramics for aeropropulsion use, Journal of the European Ceramic Society 22 (2002) 2757–2767.

[4] S. Raffaele, D.S.F. Mario, S. Laura, S. Diletta, Arc-jet testing on HfB_2 and HfC-based ultra-high temperature ceramic materials, Journal of the European Ceramic Society 28 (2008) 1899–1907.
[5] H.J. Zhou, L. Gao, Z. Wang, S.M. Dong, ZrB_2–SiC oxidation protective coating on C/C composites prepared by the vapor silicon infiltration process, Journal of the American Ceramic Society 93 (4) (2010) 915–919.
[6] Z. Wang, S.M. Dong, X.Y. Zhang, H.J. Zhou, D.X. Wu, Q. Zhou, D.L. Jiang, Fabrication and properties of C_f/SiC–ZrC composites, Journal of the American Ceramic Society 91 (10) (2008) 3434–3436.
[7] Q.G. Li, H.J. Zhou, S.M. Dong, Z. Wang, P. He, J.S. Yang, B Wu, J.B. Hu, Fabrication of a ZrC–SiC matrix for ceramic matrix composites and its properties, Ceramics International 38 (2012) 4379–4384.
[8] Q.G. Li, S.M. Dong, Z. Wang, P. He, H.J. Zhou, J.S. Yang, B. Wu, J.B. Hu, Fabrication and properties of 3D Cf/SiC–ZrC composites, using ZrC precursor and polycarbosilane, Journal of the American Ceramic Society 94 (4) (2012) 1216–1219.
[9] Q.G. Li, H.J. Zhou, S.M. Dong, Z. Wang, J.S. Yang, B. Wu, J.B. Hu, Fabrication and comparison of 3D C_f/ZrC–SiC composites using ZrC particles/polycarbosilane and ZrC precursor/polycarbosilane, Ceramics International 38 (6) (2012) 5271–5275.
[10] W.W. Wu, G.J. Zhang, Y.M. Kan, P.L. Wang, K. Vanmeensel, J. Vleugels, O.V. Biest, Synthesis and microstructural features of ZrB_2–SiC-based composites by reactive spark plasma sintering and reactive hot pressing, Scripta Materialia 57 (2007) 317–320.
[11] S. Guo, T. Nishimura, Y. Kagawa, Prepartion of zircinium diboride ceramics by reactive spark plasma sintering of zirconiun hydride–boron powders, Scripta Materialia 65 (2011) 1018–1021.
[12] J. Zhou, G.J. Zhang, Y.M. Kan, P.L. Wang, Pressureless densification of ZrB_2–SiC composites with vanadium carbide, Scripta Materialia 59 (2008) 309–312.
[13] H. Zhang, Y.J. Yan, Z.R. Huang, X.J. Liu, D.L. Jiang, Pressureless sintering of ZrB_2–SiC ceramics: the effect of B_4C content, Scripta Materialia 60 (2009) 559–562.
[14] S.M. Zhang, S. Wang, Y.L. Zhu, Z.H. Chen, Fabrication of ZrB_2–SiC-based composites by reactive melt infiltration at relative low temperature, Scripta Materialia 65 (2011) 139–142.
[15] Q. Qu, X.H. Zhang, S.H. Meng, W.B. Han, C.Q. Hong, J.C. Han, Reactive hot pressing and sintering characterization of ZrB_2–SiC–ZrC composites, Materials Science and Engineering: A 491 (2008) 117–123.
[16] X.H. Zhang, Q. Qu, J.C. Han, W.B. Han, C.Q. Hong, Microstructure features and mechanical properties of ZrB_2–SiC–ZrC composites by hot pressing and reactive hot pressing, Scripta Materialia 59 (2008) 753–756.
[17] P. Kolodziej, J. Salute, D.L. Keese, First flight demonstration of a sharp ultra-high temperature ceramic nosetip, NASA TM-112215, 1997.
[18] M. Loomis, G. Plamer, Pre-flight CFD analysis of art jet and flight environments for the SHARP-B2 flight experiment, AIAA 2001-0982, 2001.